Received: 25 July 2023 | Revised: 20 October 2023 | Accepted: 20 October 2023

DOI: 10.1111/jace.19581

Journal of the American Ceramic Society

RESEARCH ARTICLE

Optimizing raw material composition to increase sustainability in porcelain tile production: A simulation-based approach

Carine Lourenco Alves[1] | **Vasyl Skorych**[1] | **Agenor De Noni Jr**[2] | **Dachamir Hotza**[2,3] | **S. Y. Gómez González**[2] | **Stefan Heinrich**[1]

[1]Institute of Solids Process Engineering and Particle Technology, Hamburg University of Technology (TUHH), Hamburg, Germany

[2]Department of Chemical Engineering (EQA), Federal University of Santa Catarina (UFSC), Florianópolis, Santa Catarina, Brazil

[3]Graduate Program in Materials Science and Engineering (PGMAT), Federal University of Santa Catarina (UFSC), Florianópolis, Santa Catarina, Brazil

Correspondence
Carine Lourenco Alves, Institute of Solids Process Engineering and Particle Technology, Hamburg University of Technology (TUHH), 21073 Hamburg, Germany.
Email: carine.lourenco.alves@tuhh.de

Funding information
German Research Foundation, Grant/Award Numbers: 418788750, DFG DO 2026/6-1; DFG Graduate School GRK; Processes in natural and technical particle fluid systems (PintPFS), Grant/Award Number: 390794421; CAPES-DFG program, Grant/Award Number: 88881.207634/2018-01; DAAD ProBral, Grant/Award Number: 57447192

Abstract

Reducing the environmental impact of porcelain tile production while maintaining cost-effectiveness is challenging. This work introduced a novel modeling approach for optimizing a standard composition range comprising kaolinite (15–38 wt.%), illite (0–20 wt.%), quartz (20–40 wt.%), and feldspar (20–45 wt.%) to establish a robust composition interval for porcelain stoneware tiles. The proposed study considers several factors, such as composition impact on the manufacturing sequence, production costs, and CO_2 emission. A flowsheet simulation database was generated by coupling the Dyssol framework with MATLAB. This study investigated the influence of raw material composition within the process sequence, the total CO_2 emissions, and production costs within the contexts of Spain and Brazil, two of the top five global producers. Granules with a higher proportion of talc and illite exhibit reduced moisture content after spray drying, and these combinations have lower green body porosity after compaction. The addition of talc allowed for decreased porosity content after compaction reduced firing temperature, and lowered costs and CO_2 emissions despite the higher prices associated with talc. The proposed simulation methodology offers a powerful decision-making tool for optimizing raw material composition to minimize cost and CO_2 emissions in the porcelain tile production. This methodology represents an early stride toward integrating digital twin methodologies within the ceramic tile sector, facilitating improved process regulation, and promoting the adoption of digital technologies.

KEYWORDS
digitalization, optimization, porcelain tile, simulation

1 | INTRODUCTION

Porcelain tiles are part of traditional ceramics and, by definition, are a very compact product, that is, vitrified all the way through and has extremely low porosity. The final total porosity of the product ranges from 3% to 6%, in which < 1.2% is open porosity directly associated with water absorption. According to ISO13006:2018, this water absorption should be less than 0.5%.[1] This low porosity is essential because it gives the material excellent mechanical and chemical properties, making it frost-resistant and thus ideal for outdoor flooring and wall cladding in cold climates.[2]

Characteristically, porcelain tiles comprise a vitreous phase that disperses remaining minerals, such as quartz and feldspars, and freshly created phases, like mullite. The industry's ceramic tiles composition typically comprises a glassy phase comprising 40–75 wt.% of the overall matrix. This matrix incorporates quartz particles in a 10–30 wt.% ratio, mullite crystals at 4–10 wt.%, and unmelted feldspar dispersed, ranging from 0–15 wt.%.[2–4] This quantitatively dominant vitreous phase governs viscous flow sintering and significantly impacts the geometrical properties of tiles and their mechanical, tribological, and functional properties.[4] De Noni et al.,[3] in particular, reported that 14–17 wt.% mullite is best suited for achieving a robust microstructure in porcelain tiles produced using the standard industrial-scale technology. To achieve this characteristic, it is necessary to prepare a mixture of compounds. The starting composition is a triaxial mixture of clay or kaolin, quartz, and feldspar.

During ceramic tiles' processing, the clay fraction plays a vital role by providing plasticity and dry mechanical strength to the material. Upon firing, the clay transforms and develops mullite and glassy phases, further enhancing the properties of the tiles. Feldspars (primarily sodium feldspar) form glassy phases at low temperatures, assisting the sintering process and allowing for virtually zero (0.5%) open porosity and a low level of closed porosity (10%). Because of its high melting point, quartz promotes thermal and dimensional stability.[2] When raw materials are combined in the ceramic tile production, the resulting mineralogical composition typically consists of the following proportions: 20–45% kaolinite, 7–10% illite–mica, 40–50% feldspathic phases, and 15–30% quartz.[2–5] Furthermore, materials such as talc, calcite, dolomite, and diopside are added to reduce the sintering temperature.[6] Figure 1 depicts the compositions of triaxial ceramic products in which a standard composition of porcelain tile is located:

Designing porcelain tile compositions in the industry is complex and time-consuming. Raw materials modified or in different conditions will impact the final product and

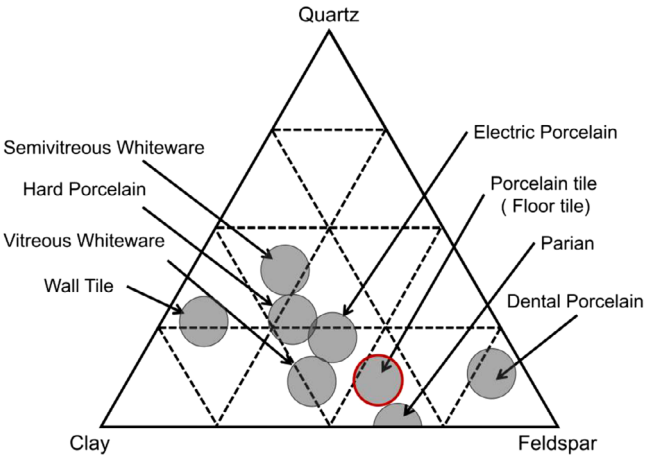

FIGURE 1 Diagram of triaxial ceramic product compositions, including porcelain tile.

the processing parameters, affecting the entire processing sequence. Porcelain tiles are manufactured through a series of processing steps that encompass three main stages: (1) wet milling and homogenization of raw materials, followed by spray-drying of the resulting suspension; (2) uniaxial pressing at 35−45 MPa of the spray-dried powder with a moisture content of 5−7 wt%; (3) thermal treatments as drying and firing. This last stage is crucial as sintering occurs during firing, resulting in maximum densification of the tiles.

The entire process consumes a large amount of thermal energy from natural gas combustion. Typically, natural gas accounts for ~92% of the sector's total energy demand, and the remaining ~8% corresponds to electric energy consumption.[2] Spray drying of the slurry accounts for ~36% of total thermal consumption, drying of newly formed tile bodies (known as green tiles) accounts for ~9%, and tile firing accounts for ~55%—the highest within the manufacturing process.[7,8] Furthermore, electrical energy is used at all stages of the process. Milling consumes the most electrical power, accounting for nearly 22% of the total consumption.[7,9] The electrical energy consumption of the milling unit is directly correlated with the milling time, which depends on the composition and original particle size distribution of the raw materials.[10–12]

On average, CO_2 emissions from natural combustion in porcelain tile manufacturing industries are estimated to be around 265 kg CO_2/t fired tile.[8] The industry's high CO_2 emissions are a concern, mainly since the European Commission published the "Roadmap for Moving to a Competitive Low-Carbon Economy in 2050" in 2011, intending to reduce CO_2 emissions by 83%–87% by the year 2050.[13,14] The ceramic tile industry is compelled to reduce emissions to maintain competitiveness amidst global climate legislation. As a result, sustainability in production has become a key research area. The industry aims to

develop strategies for emission reduction and implement sustainable practices to meet environmental goals and ensure long-term viability.

Implementing a circular economy by reusing internal production waste and waste from other production processes is considered a highly valuable approach. Several investigations have been conducted to explore the utilization of industrial waste and alternative raw materials in the manufacturing process of porcelain tiles.[15] Studies conducted by Torres et al.[16] investigated the impact of quartzite and granite sludges on the compositions of ceramic floor tiles. The findings of this study indicate a positive correlation between flexural strength values and a decrease in water absorption. The study conducted by Tarhan et al.[17] examined the potential impacts of incorporating vitrified sanitaryware waste (VSW) at different proportions to replace pegmatite and feldspar in producing glazed porcelain tiles. The study's findings demonstrate that including VSW reduces the thermal expansion coefficients. This suggests that the incorporation of VSW can result in the production of final products characterized by enhanced dimensional stability and favorable deformation properties.[17]

The integration of waste reuse into the production process of porcelain tiles holds promise in the pursuit of sustainability and the reduction of environmental impact. Numeral simulations present a viable avenue for achieving this objective. Manufacturers can assess the viability of integrating by-products and waste materials into the production cycle by applying simulation methodologies. This approach mitigates the environmental impact by decreasing waste generation and enhances cost-efficiency.

In recent years, numerical simulations have become essential for designing and optimizing industrial machinery and analyzing operation parameters. Alves et al.[10,11,18] demonstrated that flowsheet simulations could be used effectively for the process simulation of porcelain tile manufacturing and to simulate the entire plant. The flowsheet Dyssol framework[19,20] was used to implement models for each unit of porcelain tiles manufacturing. The developed simulation has proven to be effective in analyzing the impact of critical process parameters. It considers the interdependencies between individual unit operations across the entire process chain. The coupling of Dyssol with MATLAB provided a tool for optimizing and building a digital twin of the processing sequence.[10,11] Previous studies applying the proposed methodology did not consider the complexity of composition analysis despite the reported influence of raw material composition on processing parameters in the manufacturing route. However, it is essential to acknowledge and address this complexity to obtain a more comprehensive understanding of the manufacturing process and optimize it effectively.

Chitwaree et al.[8] reported that the vitrified ceramic tiles containing 50% pottery stone and 50% recycled glass could be used to manufacture low-temperature vitrified ceramic tiles with a sintering temperature of 1050°C. The properties are compliant with the regulations. The whiteness and strength are slightly inferior compared to high-quality commercial tiles. Still, the low sintering temperature contributes to a 30% reduction in thermal energy consumption and lower emission of about 0.0350 kg of equivalent CO_2 /kg of product. The reduction in strength can be correlated with mullite formation in the composition. Alternatively, intense mineral fluxes can significantly reduce the firing temperature of batches of porcelain tiles.[21] However, these fluxes contribute to an increase in the cost of raw materials. Talc additions above 10 wt.% have also been linked to compromised sintering behaviors due to induced changes in phase composition. These fluxes directly impact the liquid phase, affecting both the melt viscosity and the relative viscosity of the bulk material.[21]

The impact of various compositions used in the industrial production of porcelain tiles was examined in this study using the coupling of Dyssol and MATLAB. De Noni Jr. et al.[3] developed the concept of the microstructure-oriented composition design for porcelain tile, which was used as the foundation for correlating the firing unit processing parameters with the various analyzed composition ranges. In the present work, the mineralogical phases under consideration included kaolinite (from 15 to 38 wt.%), illite (from 0 to 20 wt.%), quartz (from 20 to 40 wt.%), and feldspar (from 20 to 45 wt.%). The ranges used in this analysis were derived from both literature data and industrial compositions. As a simplification, the simulations assumed a high degree of purity, given the specific compounds are maintained as confidential information. This study emphasizes the potential relevance of using simulation methods in industrial settings, particularly in accurately including raw material composition and by-products in the simulation database.

The primary objective of the research was to ascertain the necessary adjustments in processing parameters concerning the formulation. The applied simulation approach proved to be successful in determining these alterations. The study evaluated the potential cost reduction and improvement in process sustainability, particularly in CO_2 emissions reduction, by examining the effects of modifications in raw material composition using simulations.

2 | METHODS

Based on Alves et al.,[10,11,18] flowsheet models for each processing unit of the manufacture of porcelain tiles were created using the Dyssol framework. The data

TABLE 1 Lower and upper limits and properties of mineral components for the optimization analysis in the ceramic tile industry.

	Lower limit (wt.%)	Upper limit (wt.%)	$d_{50,3}$ (μm)	Bond work index (kWh/t)	Density (kg/m^3)	Specific heat (J/gK)
Kaolinite	15	38	5	11.6	2650	0.810
Illite	0	20	5	6	2750	0.775
Talc	0	10	5	6	2650	0.165
Quartz	20	40	24	16.6	2650	0.703
Feldspar	20	45	24	17.06	2600	0.750

from European industries collected by Nasetti et al.[12] were used to determine correlations between electrical energy consumption and processing parameters for each unit of the tile manufacturing sequence. Enthalpy and mass balances were applied to model the thermal energy consumption for the spray drying, drying, and firing units. To validate the simulated values obtained, thermal energy consumption thresholds from Nasetti et al.[12] were used.

The lower and upper limits for the mineral components for the optimization analysis were based on composition data from the literature[22–24] and industrial compositions from companies in Brazil, Italy, Spain, and Argentina.[3] Table 1 shows the range of each mineral component, average particle size ($d_{50,3}$), Bond Work Index (BWI), and density. The BWI defines ore grindability as crushing resistance, correlated to material mechanical properties defined as the kilowatt-hours per short ton required to break from infinite size to a product size of 80% passing through a 100 μm sieve.[25] Those data were added to the material database for the flowsheet simulations. They will influence the models of each processing unit within the simulation. The data from De Noni Jr[5] for kaolin (Super Standard Porcelain, Imerys, UK), quartz (SE100, Sibelco, Spain), and floated sodium feldspar (Kaltun, Turkey) were used for kaolinite, quartz, and feldspar, respectively. As an approximation, it was assumed that the average particle size of illite and talc is the same as that of kaolinite.[6,21] The sample's density and specific heat capacity vary depending on its purity, source, and location. Based on the literature datasheets for the components, an approximation of the average value for each component's density, BWI, and specific heat capacity was adopted.[3,26,27] As an important highlight, the model based on the mineral components and properties can be adjusted based on the raw material phase composition. As a result, the inclusion of by-products can also be considered in the simulation. As a first guess, the by-product composition can be deployed and addressed as equivalent to those phases already available in the implemented model. Further, new models can be built and implemented.

During wet milling, the initial raw materials are mixed and ground. The correlations suggested by Tsakalakis et al.[28] and Morell et al.[29] served as the foundation for the flowsheet model to describe the process. The particle size after milling is given by:

$$\dot{E}_{\text{el,mill}} = 0.1169 W_i d_{50,f}^{0.193} d_{50,\text{pr}}^{-0.962} \dot{m}_p, \quad (1)$$

where $d_{50,f}$ is the initial particle size (feed material), W_i is the BWI of a specific compound, $d_{50,\text{pr}}$ is the characteristic particle size of the final product and $\dot{m}$ is the mill production. The values of the utilized BWI can be seen in Table 1. The milling time correlates with the total electrical energy consumption, as presented in Equation (5).

Following wet milling, the formed slurry is atomized during spray drying, forming droplets composed of liquid and primary particles, and their moisture content is significantly reduced, reaching approximately 7 wt%. The spray drying unit was simplified by separating it into an atomizer and a drying chamber, where droplets are formed. As a result, a model based on Walzel et al.[30] was used for the atomizer, and a model based on Ali et al.[31] was used for the drying of the granules in a counter-current flow, the porcelain tile industry's most commonly used spray drying setup.

Subsequently, the produced granules are kept in a silo for roughly 24 h to allow the moisture to be homogenized. It was assumed that moisture correlated with granule size: larger granules retained more water than smaller ones. As a result, a liquid mass transfer model based on industrial data relating the moisture content in each granule and the average moisture content after spray drying was developed.[18] The granules are shaped into green tiles by pressing after storage. The uniaxial pressing was described using a semi-empirical relationship proposed by Bal'shin et al.,[32] in which the green tile's porosity depends on the spray-dried powder's density, the applied pressure, and several semi-empirical parameters. Based on previous studies,[5,33] the model was expanded to include the dependence of porosity on the average diameter $d_{50,3}$ of primary particles after milling.

Further, drying occurs in convective dryers to reduce the moisture from 6–8 wt.% to approximately 1 wt.%. Diffusion was assumed to control how the moisture distribution

changes over time within a plate following Fick's law. For the flowsheet model of this unit, a deduced analytical solution by Henderson et al.[34,35] was used. Sintering occurs during the final processing step of firing. The porosity was modeled using the method created by Gómez et al.,[36] with the sintering stage of the firing process, is assumed to be isothermal. The tiles' bulk density (fired density) was 2.35 g/cm^3, and the final overall porosity was fixed below 5%.[5,33,37]

Experimental and commercial data were used to validate each implemented model. Alves et al.[10,11,18] established the framework for the models, materials database, and process parameters that implemented each unit's energy consumption. The thermal and electrical energy requirements of each unit were evaluated separately. The thermal requirements were determined by conducting energy and mass balances for the streams within each unit. The necessary gas flow volume for the firing unit was specifically determined using industrial data gathered by a supplier of ceramic tile equipment, SACMI.[38] The model correlates the volume of gas flow with productivity, the fuel needed to maintain the high temperature of the empty furnace, the heat produced by the fumes, and the endothermic reactions that occur during the firing of porcelain tiles[10,11]:

$$\dot{v}_{f,\mathrm{fir}} = \dot{v}_{\mathrm{ul}}^{\mathrm{FR}} + X_{\mathrm{f/p}} C\mathrm{p}_{\mathrm{f}} \left(T - T^{\mathrm{RF}}\right) \frac{\dot{m}_p}{\mathrm{LHV}} + \left(\Delta H + C\mathrm{p}\left(T - T^{\mathrm{amb}}\right)\right) \frac{\dot{m}_p}{\mathrm{LHV}}. \quad (2)$$

Here, $\dot{v}_{f,\mathrm{fir}}$ is the volume flow of the hot gas required for firing in Nm^3/h; $\dot{v}_{\mathrm{ul}}^{\mathrm{FR}}$ is the flow of gas needed to keep the empty furnace at a high temperature in Nm^3/h; T is the firing temperature in °C; T^{RF} is the reference temperature—the minimum at which firing takes place in °C; $X_{\mathrm{f/p}}$ is a mass ratio of combustion fumes and dilution air to the amount of the tiles; $C\mathrm{p}_{\mathrm{f}}$ is the average specific heat capacity at a constant pressure of combustion fumes in kcal/kg.°C; ΔH is the energy consumption due to endothermic reactions in kcal/kg, $C\mathrm{p}$ is the average specific heat capacity at a constant pressure of the tiles in kcal/kg.°C; T^{amb} is the ambient temperature assumed to be 25°C; $\dot{m}_p$ is the mass flow of tiles in kg/s; and LHV is the lower heating value of natural gas in kcal/Nm^3. The mass flow rate is converted to the quantity of square meters of tiles produced using the specific weight of the tile γ. The values of these variables were based on the industry-specific, established data of SACMI,[38,39] presented in Table 2:

To determine the composition analysis, MATLAB was utilized. Specifically, 20 values were considered for each mineral composition, evenly distributed between the defined lower and upper limits. The vectors obtained from the analysis were combined and constrained to ensure a final component sum of 100% while also ensuring that each mineral had at least 20 distinct values. In total, 4,267 composition combinations were evaluated as part of the analysis.

TABLE 2 Reference values for variables of the kiln furnace gas flow model.[38,39]

Variable		Value	Units
Reference temperature	T^{RF}	1190	°C
Specific weight of the tile	γ	20	kg/m^2
Mass ratio of combustion fumes and dilution air to the amount of tiles	$X_{\mathrm{f/p}}$	2.15	–
Specific heat capacity of combustion fumes	$C\mathrm{p}_{\mathrm{fumes}}$	0.25	kcal/kg·°C
Specific heat capacity of the tiles	$C\mathrm{p}$	0.22	kcal/kg·°C
Lower heating value of natural gas	LHV	8500	kcal/Nm^3
Endothermic reactions energy	ΔH	50	kcal/kg
Required gas flow for empty kiln	$\dot{v}_{\mathrm{ul}}^{\mathrm{FR}}$	218.52	Nm^3/h
Kiln length	L	150	m
Kiln width	w	2.5	m

The milling time and firing temperature were determined for each combination. The milling time for each combination was determined to ensure that the medium particle size of the slurry is below 6 μm, using Equation (1). The firing temperature was assessed from the empirical model developed by De Noni Jr. et al.[3] as seen in Equation (3):

$$T_{\mathrm{fir}} = 1390 - 310X_F - 1090X_I - 3150X_T + 1090X_FX_I + 4250X_FX_T + 15900X_IX_T - 21900X_FX_IX_T. \quad (3)$$

Here, T_{fir} is the firing temperature in °C and X_i are mass fractions of the phases (F feldspar, I illite, and T talc). The contribution of kaolinite and quartz phases is linked to the constant parameter 1390. The dwell time for the firing time is assumed to be 5 min at maximum temperature, and the total firing time to be 30 min. These values were based on industrial kilns and were adopted by De Noni Jr. et al.[3] to validate the proposed correlation in Equation (3). As a result, all simulations had the same productivity because the productivity is inversely proportional to the whole firing cycle time cold-to-cold t_{fir} (the sum of pre-heating, firing, and cooling time),[1140] as seen in Equation (4):

$$\mathrm{Pr} = \frac{Lw\eta_g\eta_{lr}^2}{t_f} \quad (4)$$

where L and w are the kiln length and width in meters, with values shown in Table 2. η_g is the geometry efficiency, η_{lr} is the shrinkage efficiency, and t_f is the total firing cycle time in seconds. The geometry efficiency η_g is the ratio of the area occupied by the tiles to the total area of the

furnace. It is assumed to be 0.98, considering 1 cm of spacing between longitudinal rows and 2 mm spacing between transverse rows.[41] η_{lr} is based on the linear shrinkage (lr) during firing and is assumed to be 0.93, considering the constant density of the green tile and final tile as well as fire loss.[10,11] The total production was determined as 526.75 m^2/h or 10.54 ton/h.

Since each of the 4 267 simulations lasted about 25 s, the comprehensive analysis took roughly 29 h and 40 min.

The costs include electrical and thermal energy, fixed costs, CO_2 emission taxes, raw materials, and glazing. The production costs were divided based on scenarios for Brazil and Spain, two of the top five global producers, using either a constant price for raw materials ($C_{\text{pr 1}}$) or prices for each mineral phase ($C_{\text{pr 2}}$).[42] The selection of these two scenarios is based on industrial partners from the authors and the distinction of economic factors such as electrical energy costs and CO_2 emission taxes. Consequently, for each combination, four production costs were obtained ($C_{\text{pr 1,Brazil}}$, $C_{\text{pr 2,Brazil}}$, $C_{\text{pr 1,Spain}}$ and $C_{\text{pr 2,Spain}}$). These two scenarios were chosen based on the authors' industrial partners and differences in economic factors such as electrical energy costs and CO_2 emission taxes. The values for each mineral phase were based on industrial values from Brazil, without regard for the geographical region or material contamination.[3] All costs were considered in USD for normalization.

Natural gas was used as the fuel, and its LHV was 8500 kcal/Nm^3 or 9.88 kWh/Nm^3, with estimated CO_2 emissions of 56 100 kg CO_2/TJ or roughly 0.2 kg CO_2/kWh, resulting in 1.976 kg CO_2/Nm^3 of natural gas emitted.[39,43] Additionally, electrical energy contributes to CO_2 emissions. In 2022, the average emissions of Spain were 195 g CO_2eq/kWh.[44] This value is relatively high compared to the Brazilian scenario, where the emissions intensity was 98 g CO_2eq/kWh.[45] The difference can be attributed to Spain's reliance on fossil fuels for electricity generation compared to Brazil, which has a significant hydropower and renewable energy sector. Table 3 summarizes the values for each cost component for Brazil and Spain:

As proposed by Alves et al.,[10,11] the sum of the electrical energy consumption of each unit in the processing sequence (Equation (5)) gives the total electrical energy consumption ($\dot{E}_{\text{el,total}}$)) in kWh/ton. The interplay between the mass load and the electrical energy consumption of milling, pressing, spray drying, drying, and firing is described in each unit by Equations (5)–(10), accordingly:

$$\dot{E}_{\text{el,total}} = \dot{E}_{\text{el,mill}} + \dot{E}_{\text{el,sdry}} + \dot{E}_{\text{el,press}} + \dot{E}_{\text{el,dry}} + \dot{E}_{\text{el,fir}} \quad (5)$$

$$\dot{E}_{\text{el,mill}} = 7.6\dot{m}_p t_{\text{mill}} \quad (6)$$

$$\dot{E}_{\text{el,press}} = 20\dot{m}_p \quad (7)$$

$$\dot{E}_{\text{el,sdry}} = 8\dot{m}_p \quad (8)$$

$$\dot{E}_{\text{el,dry}} = 12\dot{m}_p \quad (9)$$

$$\dot{E}_{\text{el,fir}} = 22\dot{m}_p \quad (10)$$

where $\dot{m}_p$ is the mass flow of the product that generates the final tile. The correlations were proposed by the collected data from Nassetti et al.[12] and have been previously applied in the literature.[10,11] In contrast to the other units, there is an additional factor of milling time (t_{mill}) specific to the unit.[33]

Because there is currently no CO_2 tax in Brazil, this value was not factored into the cost calculation, in contrast to European industry conditions, where CO_2 emissions taxes need to be considered.[46,47] The raw material and glazing costs in Spain were assumed to be the same as in Brazil because these values do not vary due to differences in processing parameters and thus do not influence the variation in total production cost. The glazing mass is assumed to be 10% of the total mass of the tiles.[38,39] Extra charges for staff, miscellaneous inputs, maintenance, and insurance are estimated to be 1/3 of the total production cost in both Brazil and Spain ($C_{\text{extra}} = 1/3C_{\text{pr}}$). Additionally, it is assumed that packing will cost 1/4 of the total cost of production ($C_{\text{packing}} = 1/4C_{\text{pr}}$). Equations (11)–(14) describe the various methods for calculating total production costs in Brazil ($C_{\text{pr 1,Brazil}}$) and Spain ($C_{\text{pr 1,Spain}}$), assuming constant raw material costs and the value of each mineralogical phase cost in Brazil ($C_{\text{pr 2,Brazil}}$) and Spain ($C_{\text{pr 2,Spain}}$), respectively:

$$C_{\text{pr 1,Brazil}} = \left(1 + \frac{1}{3} + \frac{1}{4}\right)\left[\gamma \text{Pr}\left(C_{\text{raw}} + C_{\text{glaz}}0.1 + C_{\text{el}}E_{\text{el,total}} + \frac{E_{\text{th,sdry}}C_{\text{sdry}}}{\text{LHV}} + \frac{E_{\text{th,dry}}C_{\text{fuel}}}{\text{LHV}}\right) + \dot{v}_{f,\text{fir}}C_{\text{fuel}}\right] \quad (11)$$

$$C_{\text{pr 1,Spain}} = \left(1 + \frac{1}{3} + \frac{1}{4}\right)\left[\gamma \text{Pr}\left(C_{\text{raw}} + C_{\text{glaz}}0.1 + C_{\text{el}}E_{\text{el,total}} + \frac{(E_{\text{th,sdry}} + E_{\text{th,dry}})C_{\text{fuel}}}{\text{LHV}}\right) + \dot{v}_{f,\text{fir}}C_{\text{fuel}}\right] + 1.976C_{\text{CO2}}\dot{v}_{f,\text{total}} \quad (12)$$

$$C_{\text{pr 2,Brazil}} = \left(1 + \frac{1}{3} + \frac{1}{4}\right)\left[\gamma \text{Pr}\left(X_F C_{\text{raw,F}} + X_k\, C_{\text{raw,K}} + X_I C_{\text{raw,I}} + X_q C_{\text{raw,Q}} + X_t C_{\text{raw,T}} + C_{\text{glaz}}0.1 + C_{\text{el}}E_{\text{el,total}} + \frac{E_{\text{th,sdry}}C_{\text{sdry}}}{\text{LHV}} + \frac{E_{\text{th,dry}}C_{\text{fuel}}}{\text{LHV}}\right) + \dot{v}_{f,\text{fir}}C_{\text{fuel}}\right] \quad (13)$$

TABLE 3 Unit costs for raw materials, electrical energy, fuel, and CO_2 emissions taxes for Brazil and Spain.

Costs	Brazil	Spain	Units
Constant raw material (C_{raw})	28.5	28.5	USD/ton
Feldspathic phase ($C_{raw,F}$)	70	70	USD/ton
Kaolinite ($C_{raw,K}$)	15	15	USD/ton
Illite ($C_{raw,I}$)	10	10	USD/ton
Quartz ($C_{raw,Q}$)	5	5	USD/ton
Talc ($C_{raw,T}$)	40	40	USD/ton
Glazing (C_{glaz})	475	475	USD/ton
Electrical energy (C_{el})	0.0665	0.0497	USD/kWh
Spray drying (C_{sdry})	0.076	0.0606	USD/kg of dried material
Fuel (C_{fuel})	0.7733	1.5609	USD/Nm^3
Electrical CO_2 emissions ($C_{el,CO2}$)	1.95e−4	9.8e−5	ton CO_2/kWh
Taxes on CO_2 emissions (C_{CO2})	–	16.58	USD/ton CO_2

$$C_{\text{pr 2,Spain}} = \left(1+\frac{1}{3}+\frac{1}{4}\right)\left[\gamma \text{Pr}\left(X_F C_{\text{raw},F} + X_k\, C_{\text{raw,K}} + X_I C_{\text{raw,I}} + X_q C_{\text{raw,Q}} + X_t C_{\text{raw,T}} + C_{\text{glaz}} 0.1 + C_{\text{el}} E_{\text{el,total}} + \frac{(E_{\text{th,sdry}} + E_{\text{th,dry}}) C_{\text{fuel}}}{\text{LHV}}\right) + \dot{v}_{f,\text{fir}} C_{\text{fuel}}\right] + 1.976 C_{CO2} \dot{v}_{f,\text{total}}. \quad (14)$$

This assessment evaluated the costs by considering the total cost per square meter of produced porcelain tile (USD/m^2). The sustainability of the process sequence was assessed based on the total CO_2 emissions. Prices in US dollars were calculated using the following exchange rates: 0.19 USD/R$ and 0.98 USD/€.

3 | RESULTS AND DISCUSSION

Talc received particular attention in the analysis due to its distinctive physical characteristics, including softness, lubricity, and low abrasiveness. These properties make talc an important additive in the ceramic tile manufacturing process. Additionally, talc functions as a flux agent, reducing sintering temperatures and promoting densification.[6,21,48,49] As a result, careful monitoring of the talc concentration should guarantee the porcelain tiles' performance, cost-effectiveness, and properties during production.

Milling time, spray-dried granule moisture, green body porosity, and sintering temperature vary with composition. The evaluation of each property results in a multidimensional analysis. Colormaps were created for each component (kaolin, quartz, feldspar, and illite) with a gradient based on talc content to evaluate the effects of each composition component on these various parameters. The colormaps were created by plotting the property values concerning the different composition components with constant slices of the talc compositions and performing cubic interpolation of the values. The slurry's minimum milling time to reach at least 6 μm of medium particle size (d50,3) varied according to the composition. Figure 2 compares the minimum milling time for different compositions based on the concentration of (a) kaolin, (b) quartz, (c) feldspar, and (d) illite:

Milling time increases proportionally to feldspar content and decreases proportionally to illite and talc content. The shortest milling time was determined for a composition consisting of 20 wt.% feldspar, 23.59 wt.% quartz, 29.74 wt.% kaolin, 8.72 wt.% talc, and 17.95 wt.% illite, the shortest milling time. On the other hand, the maximum milling time was determined for a composition of 42 wt.% feldspar, 28.2 wt.% quartz, 20.3 wt.% kaolin, 0.26 wt.% talc, and 9.23 wt.% illite. The range of milling time was from 11.76 to 13.97 h. These milling times are commonly associated with achieving a particle size distribution with a $d_{50,3}$ of approximately 6 μm for the slurry.[10,11,33] It was assumed that the average density of each component within the composition was similar. Additionally, it was assumed that changes in composition would not significantly impact the properties of the slurry obtained after milling. As a result, the composition variation influences the entire process sequence. Figure 3 compares the composition influence on the moisture of the obtained granules after spray drying:

While illite reduced the moisture content of the granules after spray drying, the increase in quartz content contributed to the increase in moisture content. This finding contrasts the hydrophilic properties of illite and the hydrophobic nature of quartz, suggesting that illite has an innate tendency to attract and retain water molecules, hence promoting moisture absorption.

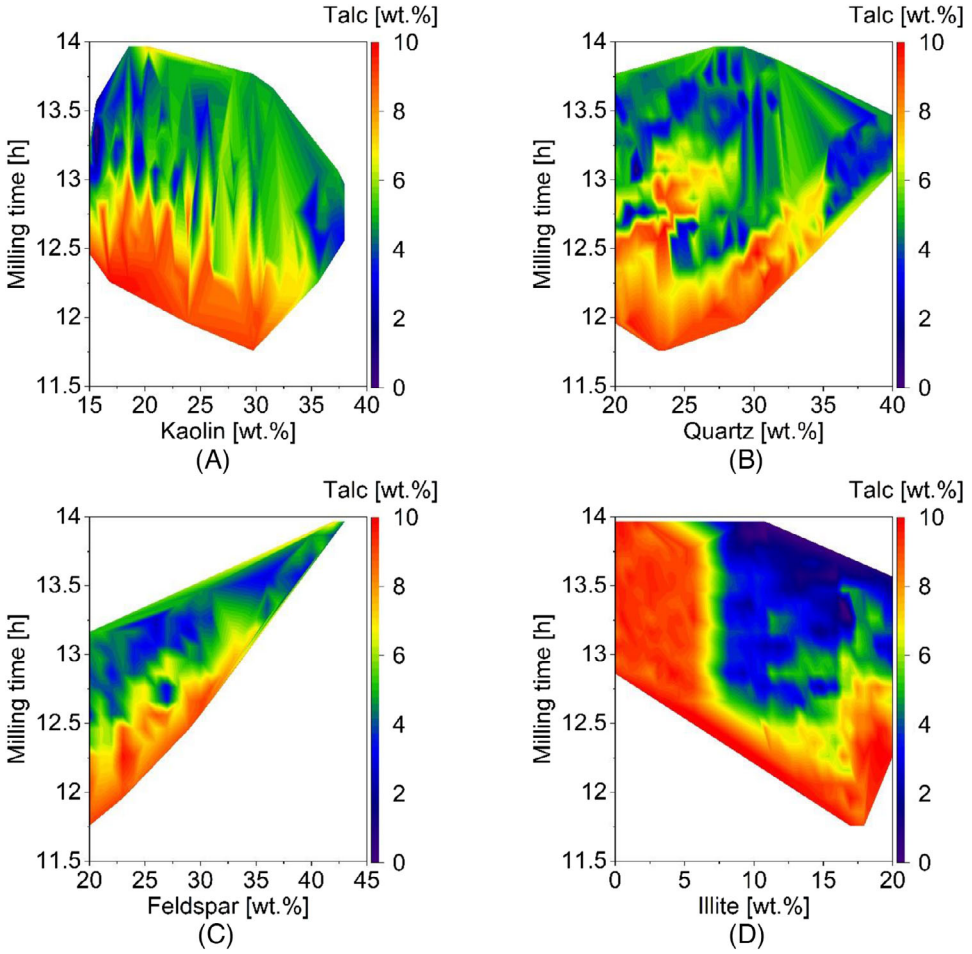

FIGURE 2 Comparison of minimum milling time according to the content of (A) kaolin, (B) quartz, (C) feldspar, and (D) illite.

The justification for the influence of compounds on the particle size distribution of the slurry during milling may be derived from the modeling of spray drying kinetics. The distribution of particle sizes affects the drying process because smaller sizes have a longer residence time and a larger specific surface area, which causes them to lose moisture more quickly than larger sizes. The same has been reported in the literature.[50,51] Additionally, the granules' moisture content is decreased through elevated temperatures and airflow during the spray drying procedure. In the presence of a notable concentration of illite, the moisture that the granules have absorbed may exhibit a gradual release while the granules undergo the drying process. The progressive release of moisture can mitigate the hydrophilic properties of illite, resulting in a reduced overall moisture content in the end product.

Although not explicitly discussed in the simulation, previous studies have indicated that the inclusion of illite content in granules may have the ability to increase their porosity.[52,53] The water-absorbing properties of illite may result in the formation of more holes and increased surface area within the granules. The presence of these pores enables the illite to function as a moisture reservoir, facilitating the absorption and retention of water within the granules. Hence, although the simulation outcomes may be deemed justifiable, it is advisable to undertake experimental research to evaluate the data derived from those simulations.

The moisture content, however, varies between 6.86 wt.% and 7.19 wt.%, indicating a variance of only 0.33 wt.%. This difference does not lead to very substantial changes in the compaction of the parts. Currently, industrial facilities regulate the moisture content levels of atomized powder to ensure that it remains within a specified maximum variation range of 1 wt.%.[54–57] Yet, achieving this target can be challenging. Thus, the suggested simulations can be useful to demonstrate how this might be attained in a more straightforward method, reducing experimental trials.

The porosity after pressing (green body porosity) is compared with various combinations of raw materials in Figure 4.

The green body porosity ranged from 29.68% to 30.72%, decreasing with increasing talc content. Increasing the

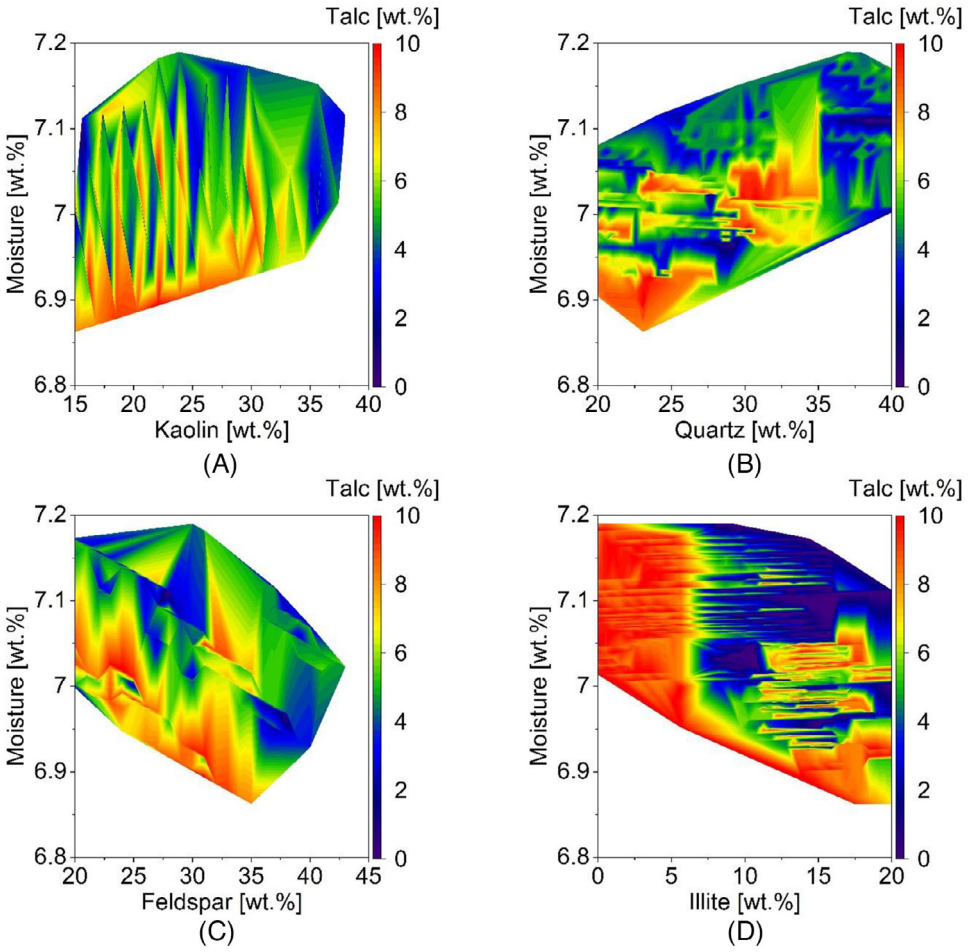

FIGURE 3 Comparison of granules moisture after spray drying according to the content of (A) kaolin, (B) quartz, (C) feldspar, and (D) illite.

proportion of quartz in a composition can increase porosity after compaction. Talc has a platy or flake-like shape, which can reduce the porosity of porcelain tiles after pressing. The talc particles can align themselves during pressing, creating a "barrier" that limits the space for other particles in the tile formulation to move. The talc particles' alignment results in a more compact structure that lessens the quantity and size of pores in the green tile.[6,21]

Additionally, the surface energy of talc particles is relatively low, which can lessen the surface tension between the particles in the formulation of the tile. As a result, the particles may be packed more uniformly, which may also reduce the porosity of the tile.[48,49] The same has been concluded by Darolt et al.[33] and Ishizaki et al.[58]

The effect of raw material composition on the processing sequence demonstrates how the proposed simulation methodology applies to the entire manufacturing line and is adaptable to variations in raw material conditions. In Figure 5, color maps display the determined sintering temperatures for different compositions based on the concentration of the compounds.

The composition of 23.00 wt.% feldspar, 30.77 wt.% quartz, 36.23 wt.% kaolin, 10.00 wt.% talc, and 0 wt.% illite exhibited the lowest firing temperature of 1101.45°C. The maximum sintering temperature was determined to be 1252.04°C for a combination of 22 wt.% feldspar, 31.8 wt.% quartz, 38 wt.% kaolin, 0 wt.% talc, and 8.2 wt.% illite. As previously observed in the literature, the sintering temperature decreases with the talc content,[6,21] leading to a difference of nearly 150°C. The firing temperature is closely connected to the melting temperatures and reactivity of the components that make up ceramic compositions. Due to common fluxing agents, the ceramics system can present a lower melting point and vitrify at lower temperatures. On the other hand, refractory materials with higher melting points, including quartz and kaolin, may be employed.[3,59] The interactions between different components may produce synergistic effects. Illite, for instance, is renowned for its plasticity and may impact how the ceramic mixture compacts and fuses. It could interact with other elements, such as kaolin, in ways that affect the firing temperature as a whole.[60] The simulation results were

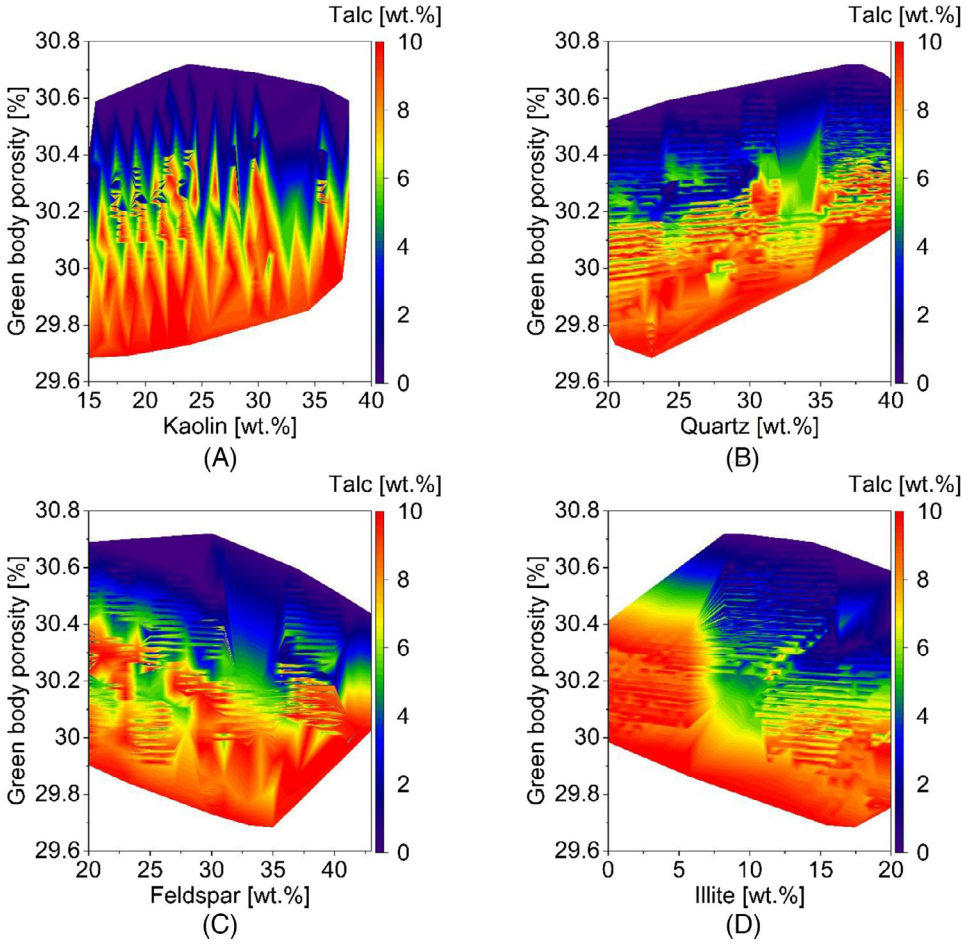

FIGURE 4 Comparison of porosity after pressing according to the content of (A) kaolin, (B) quartz, (C) feldspar, and (D) illite.

derived from the proposed correlation by De Noni Jr. et al.,[3] which was formulated using data obtained from industry plants. The suggested composition range guaranteed the mullite production, producing a strong microstructure for porcelain stoneware tiles using standard industrial-scale techniques.

To ascertain the actual influence of these changes in composition on the firing temperature, it is recommended to carry out empirical investigations. However, the suggested simulation approach serves as a crucial decision-making tool for adjusting processing parameters and identifying particular experiments that should be undertaken to limit the number of needed trials. This is particularly valuable when considering an extensive range of spatial combinations.

The sintering temperature and CO_2 emissions are directly related. This can be observed in Figure 6, considering the Brazilian scenario.

CO_2 emissions ranged from 8.66 kg/m^2 (4.56 ton/h) to 10.01 kg/m^2 (5.27 ton/h), a 0.71 ton/h difference of CO_2. The contribution of CO_2 emissions due to electrical energy in Spain ranged from 5.83×10^{-5} to 6.59×10^{-5} ton/h, while in Brazil, it went from 2.93×10^{-5} to 3.31×10^{-5} ton/h. As a result, no graphic variation between the Spanish and Brazilian scenarios for CO_2 emissions can be observed. This can be explained by the fact that electrical energy contributes less than thermal energy for the porcelain tile manufacturing route.

Including talc in the raw material composition has led to a significant cost increase, particularly due to the higher cost associated with this component (Table 3).[6,26] Considering raw materials costs as a constant value, Figure 7 compares the total cost of production and CO_2 emissions for Spain ($C_{pr\ 1,Spain}$) and Brazil ($C_{pr\ 1,Brazil}$).

The total cost of production and CO_2 emissions for various raw material combinations in Spain ($C_{pr\ 2,Spain}$) and Brazil ($C_{pr\ 2,Brazil}$) can be seen in Appendix A. The increased talc content reduced both scenarios' total production costs and CO_2 emissions. Although the number of generated data points is the same for both systems, the data for the Spanish scenario are divided into more line segments than the Brazilian scenario. This segmentation indicates that the Spanish data are more concentrated, suggesting a narrower range of variation compared to the

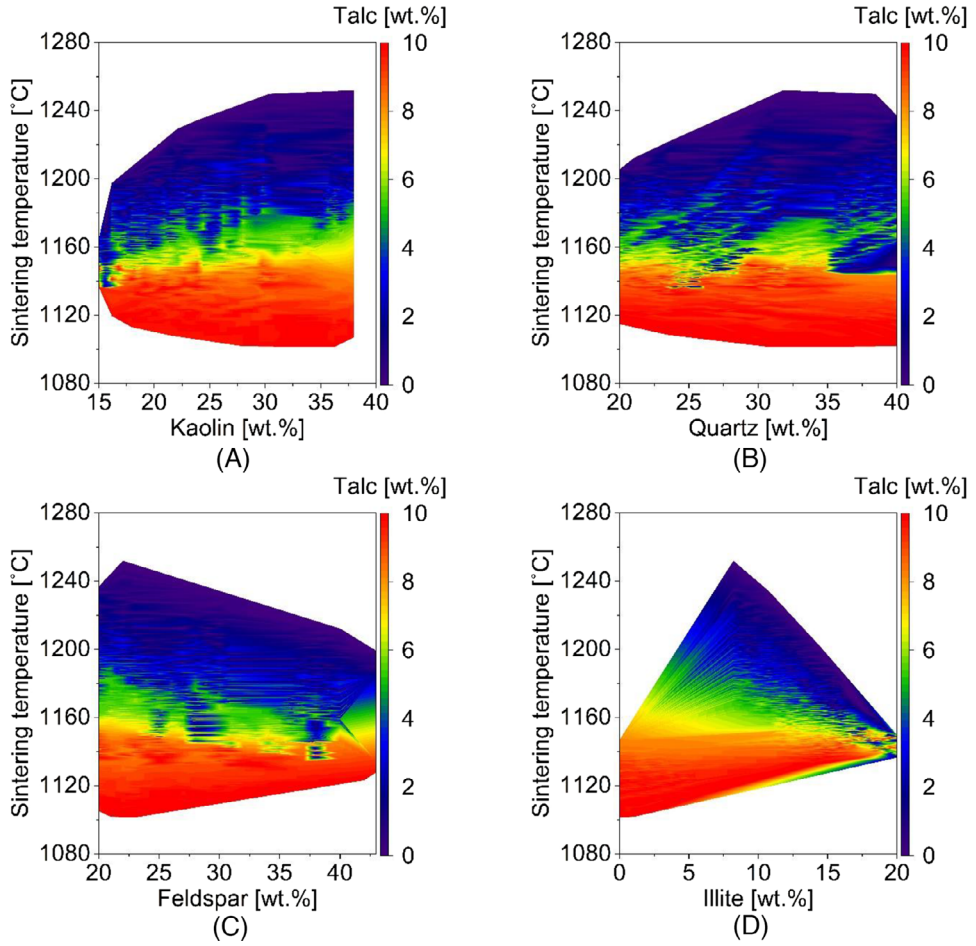

FIGURE 5 Comparison of sintering temperature according to the content of (A) kaolin, (B) quartz, (C) feldspar, and (D) illite.

Brazilian data. The concentration of data points in the Spanish scenario may be attributed to factors such as CO_2 taxes and higher electrical energy costs. These cost-related factors could lead to more focused and consistent data, as they likely influence the decision-making process and incentivize a more concentrated range of compositions or process optimizations.

Figure 8 compares the CO_2 emissions and total costs in the Brazilian scenario considering the raw material costs ($C_{pr\ 2,Brazil}$), talc content, and sintering temperatures. The lowest costs can be seen to correspond with the lowest CO_2 emissions and highest talc contents. The cost range for Spain is between 6.53 and 7.08 U$/m^2, while for Brazil, the range is between 4.22 and 4.58 US$/m^2. This variation can be explained by the CO_2 tax emission already placed for Spain. As a result, using fluxes such as talc, which contributes to lower CO_2 emissions and costs, has a more significant impact in Spain than in Brazil. Another important consideration is that the assumed costs for raw materials were determined based on the prices of the mineralogical phases rather than the individual compounds themselves. This approach reflects the industry practice of evaluating and pricing raw materials based on their mineralogical composition rather than their elemental or compound composition. In practice, the raw materials for porcelain tile manufacturing are obtained through compounds containing different mineralogical phases with varying degrees of purity, directly reflecting the raw material costs. Furthermore, prices for both Spain and Brazil were averaged, even though raw material prices are heavily influenced by location. Overall, the initial analysis using these values laid the groundwork for assessing the simulation methodology's capabilities and provided valuable information on the implications of changing the raw material composition within the ceramic tile manufacturing process.

4 | CONCLUSIONS

Porcelain tiles are manufactured using a combination of mineral raw materials. Typically, these materials include 20–45% kaolinite, 7–10% illite–mica, 40–50% feldspathic phases, and 15–30% quartz. In the industry,

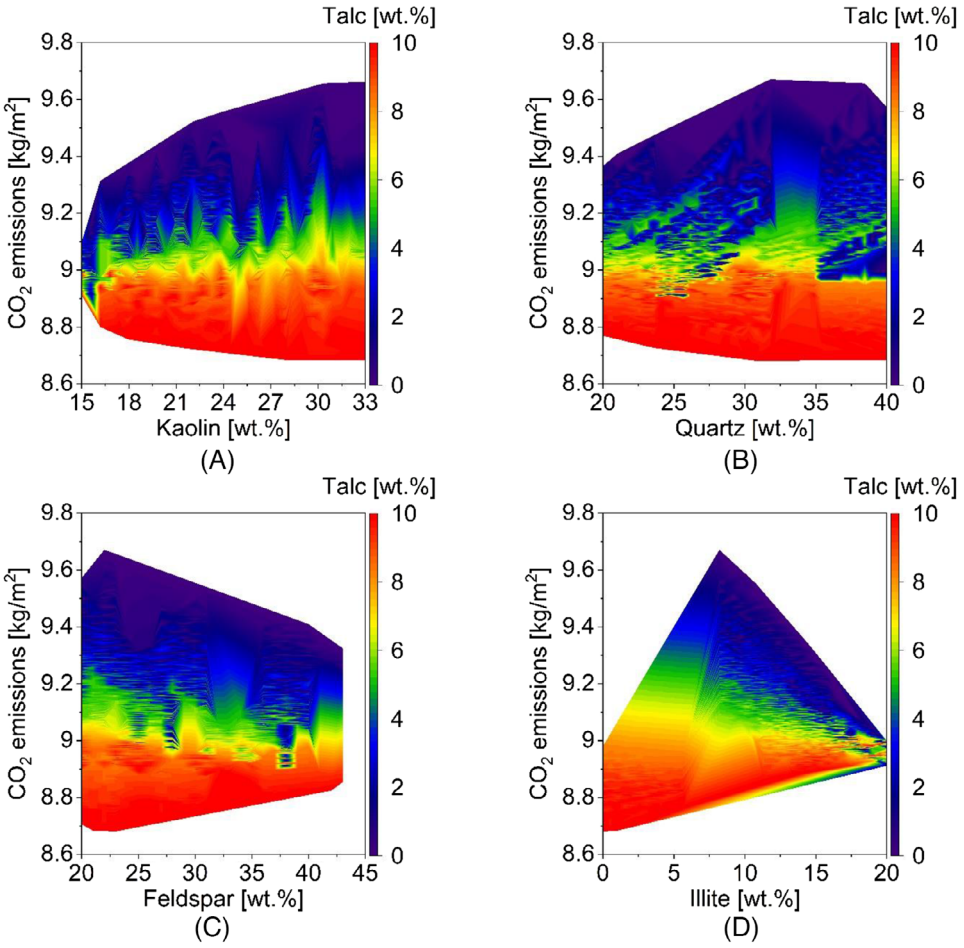

FIGURE 6 Comparison of CO_2 emission from the Brazilian scenario according to the content of (A) kaolin, (B) quartz, (C) talc, (D) feldspar, and (E) illite.

the composition design is a complex and time-consuming task. Environmental concerns are driving an increase in demand for CO_2 emission reductions. To tackle these challenges, the developed simulation methodology was expanded to incorporate the composition of kaolinite, illite, feldspar, and quartz raw materials. This was achieved by utilizing flowsheet simulations with the Dyssol framework and coupling it with MATLAB. By integrating the composition data into the simulation framework, the analysis could capture the influence of varying compositions on the overall process and its outcomes.

The minimum required milling time for the various material combinations to produce a slurry with at least a median particle size of 6 μm was calculated using simulations. Similarly, semi-empirical correlations determined specific sintering temperatures for each raw material combination. Simulations were used to correlate total CO_2 emissions and total production costs, considering both the Brazilian and Spanish scenarios, with a constant value for raw materials and the cost of each mineralogical phase. In total, 3 864 simulations were performed for the analysis.

The modifications made to the raw materials within the ceramic tile manufacturing process can be observed in the total costs and the resulting variations in CO_2 emissions. These modifications have an impact on multiple stages throughout the entire process sequence. The milling time required to achieve a minimum median particle size of 6 μm increases proportionally to feldspar and quartz amount and decreases proportionally to illite, kaolin, and talc content. The granules formed from more talc and illite combinations have less moisture after spray drying, and these combinations have lower green body porosity after compaction. This can be explained by smaller particles having a longer residence time and a larger surface area than larger particles, contributing to more moisture loss. Talc particles can also align to ensure greater compactability due to their flake-like shape.

Even though talc has been associated with higher prices, this flux contributes to lowering total production costs and CO_2 emissions in both Brazilian and Spanish scenarios. The raw material costs were estimated and averaged based on the mineralogical phases, with no regard for cost

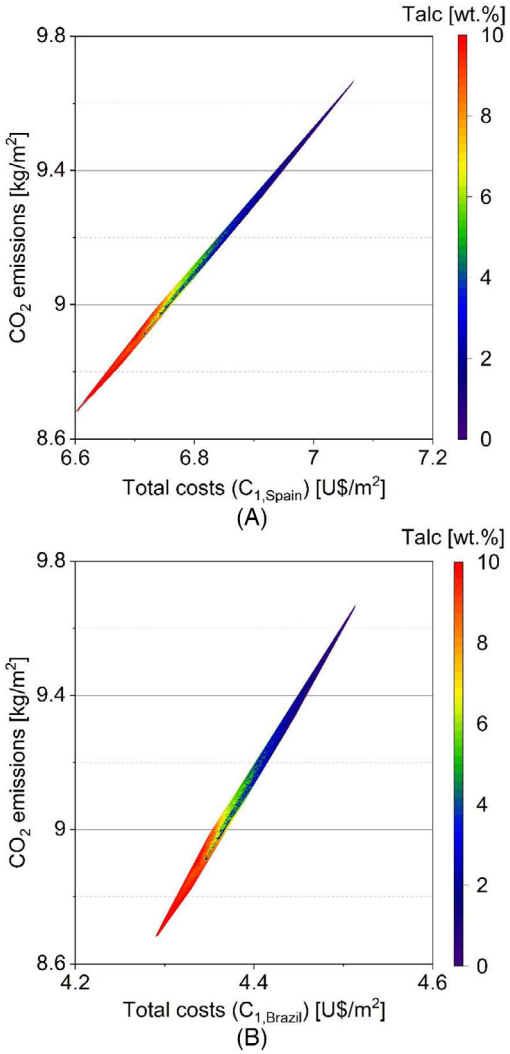

FIGURE 7 Comparison of total costs production with CO_2 emissions considering raw material costs as constant for (A) Spain, and (B) Brazil.

variation based on location. While the exact production costs may vary due to market fluctuations and specific operational considerations, the simulation incorporated cost approximations to provide a more accurate representation of the economic implications of the raw material modifications.

The improvement of the proposed simulation methodology proved effective in predicting the outcome of both modified process parameters and raw material start composition in manufacturing porcelain tiles. The simulation approach's application potential can be broadened by integrating by-products, waste materials, or dry raw materials. The raw materials can be subject to modification following specific requirements. Also, additional recycling streams can be implemented to enhance waste management practices. Specifically, the proposed simulation methodology enables the prediction of the consequences of employing dry raw materials and anticipating fluctuations in the manufacturing process and product quality throughout the manufacturing sequence. Manufacturers can utilize the simulation methodology to evaluate the feasibility of incorporating by-products, waste materials, and dry raw materials into the production cycle. This approach will not only serve to reduce the environmental impact by decreasing waste generation but also enhance cost-effectiveness without compromising the quality of the product.

The simulation methodology holds significant applicability in decision-making even before purchasing raw materials and modifying the manufacturing sequence. Using the simulation to evaluate various compositions, manufacturers can assess the optimal raw material composition that minimizes production costs and CO_2 emissions. This process allows manufacturers to make informed decisions on revalorizing waste and potentially replacing or supplementing traditional raw materials with more sustainable alternatives.

The proposed methodology has demonstrated promising capabilities in digitizing the entire process sequence of porcelain tile manufacturing. By creating a digital twin of the manufacturing chain, the methodology enables virtual representation and analysis of the production process, yielding several notable benefits. The proposed simulation methodology has the potential to boost production efficiency through the implementation of real-time monitoring and control, resulting in reduced downtime and the elimination of errors. The method allows for modeling and optimizing several processing units, facilitating the detection of bottlenecks and inefficiencies before interference with the tangible production line. Upon receiving various raw material compositions, distinct processing parameters can be promptly identified according to this raw material composition.

The simulation makes a significant contribution to achieving cost reductions. It allows for evaluating many situations and decision-making without complex physical modeling or costly trial and error. Quality assurance is an additional noteworthy benefit. Through constant virtual representation and analysis, manufacturers can detect defects or deviations from prescribed standards in the early stages of production, ensuring that only products of exceptional quality are introduced to the market. The matter of sustainability objectives is also being tackled. By using the optimization approaches suggested by the simulation, manufacturers have the potential to mitigate energy usage, emissions, and waste effectively, therefore aligning their production operations with ecologically sustainable principles. The approach above also enables decision-making, that is, grounded in empirical facts. The system can generate a vast amount of data that can be utilized for

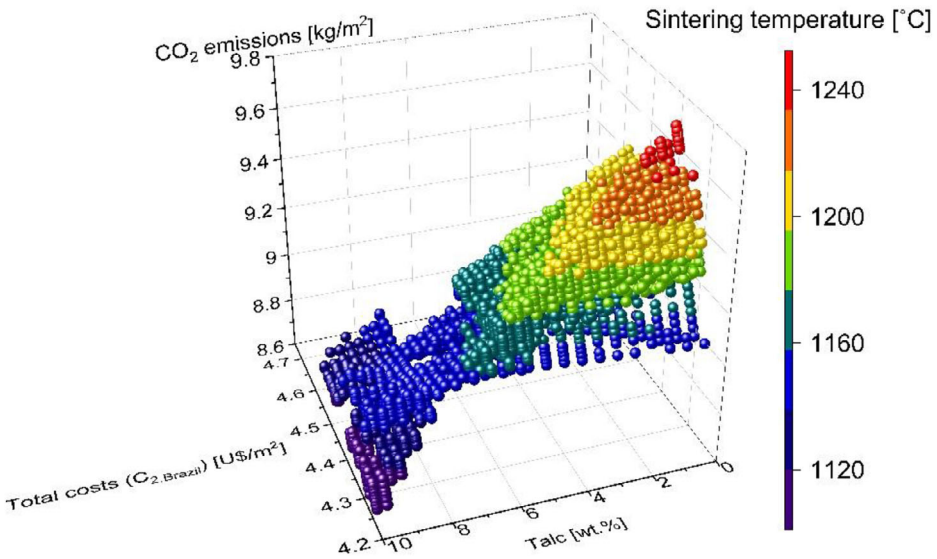

FIGURE 8 Dependence of CO_2 emissions in the Brazilian scenario with total costs (*C*_(pr 2,Brazil)), talc content, and sintering temperature.

analysis and predictive maintenance. This enables informed decision-making, forecasting of equipment repair needs, and continuous improvements in operational processes.

Overall, using the flowsheet frameworks for simulating manufacturing processes for porcelain tiles offers numerous practical benefits, including enhanced operational efficiency, cost reduction, quality assurance, increased adaptability, improved sustainability, data-driven insights, and a favorable competitive edge. The methodology facilitates the creation of a digital model. It examines the manufacturing process, introducing a new age of flexible, efficient, and ecologically sustainable manufacturing practices in the porcelain tile industry.

NOMENCLATURE

Symbol	Description	Unit
C	Cost	USD/ton
C_p	Specific heat	J/kgK
$\dot{E}_{el}$	Electrical energy consumption	kWh/ton
LHV	Lower heating value of natural gas	kcal/Nm^3
$\dot{m}$	Mass flow rate	kg/s
t	Time	h
T	Temperature	˚C
$\dot{v}_{ul}^{FR}$	Required gas flow for empty kiln	Nm^3/h
W_i	Bond work index	kWh/t
X	Mass fraction	–
$X_{f/p}$	Mass ratio of combustion fumes and dilution air	–
Greek letters		
ΔH	Endothermic reactions energy	kcal/kg
γ	Specific weight of the tile	kg/m^2
Subscripts and superscripts		
dry	Drying	
f	Feed	
F	Feldspar	
fir	Firing	
fuel	Fuel	
fumes	Fumes	
glaz	Glazing	
I	Illite	
K	Kaolinite	
mill	Milling	
pr	Product	
press	Pressing	
raw	Raw materials	
RF	Reference	
sdry	Spray drying	
T	Talc	

ACKNOWLEDGMENTS

We gratefully acknowledge the financial support of the German Research Foundation (DFG). Project ID: 418788750 (DFG DO 2026/6-1) and DFG Graduate School GRK 2462 “Processes in natural and technical particle fluid systems (PintPFS)” (Project No. 390794421) as well the DAAD (Pro Bral 57447192) and CAPES-DFG program (PIPC 88881.207634/2018-01).

Open access funding enabled and organized by Projekt DEAL.

ORCID

Carine Lourenco Alves https://orcid.org/0000-0002-7144-6152

Agenor De Noni Jr https://orcid.org/0000-0001-9713-5283

Dachamir Hotza https://orcid.org/0000-0002-7086-3085

S. Y. Gómez González https://orcid.org/0000-0003-4019-261X

REFERENCES

1. International Organization for Standardization ISO standard, ISO 13006 Ceramic Tiles. Int. CERLabs.; 2018
2. Sánchez E, García-Ten J, Sanz V, Moreno A. Porcelain tile: almost 30 years of steady scientific-technological evolution. Ceram Int. 2010;36:831–45. https://doi.org/10.1016/j.ceramint.2009.11.016
3. De Noni A Jr., Canever SB, Henrique P, da Silva RR. Microstructure-oriented porcelain stoneware tile composition design. Ceram Int. 2023;49(14):24558-65. https://doi.org/10.1016/j.ceramint.2022.11.067
4. Zanelli C, Raimondo M, Guarini G, Dondi M. The vitreous phase of porcelain stoneware: composition, evolution during sintering and physical properties. J Non-Cryst Solids. 2011;357:3251–60. https://doi.org/10.1016/j.jnoncrysol.2011.05.020
5. Noni De Jr., A, H, Dachamir, Soler VC, Vilches ES. Influence of composition on mechanical behaviour of porcelain tile. Part I: Microstructural characterization and developed phases after firing, Mater Sci Eng A. 2010;527:1730–35. https://doi.org/10.1016/j.msea.2009.10.057
6. Dondi M. Feldspathic fluxes for ceramics: sources, production trends and technological value. Resour Conserv Recycl. 2018;133:191–205. https://doi.org/10.1016/j.resconrec.2018.02.027
7. Ferrer S, Mezquita A, Aguilella VM, Monfort E. Beyond the energy balance: exergy analysis of an industrial roller kiln firing porcelain tiles. Appl Therm Eng. 2019;150:1002–15. https://doi.org/10.1016/j.applthermaleng.2019.01.052
8. Chitwaree S, Tiansuwan J, Thavarungkul N, Punsukumtana L. Energy saving in sintering of porcelain stoneware tile manufacturing by using recycled glass and pottery stone as substitute materials. Case Stud Therm Eng. 2018;11:81–88. https://doi.org/10.1016/j.csite.2018.01.002
9. Mezquita A, Boix J, Monfort E, Mallol G. Energy saving in ceramic tile kilns: cooling gas heat recovery, Appl Therm Eng. 2014;65:102–10. https://doi.org/10.1016/j.applthermaleng.2014.01.002
10. Alves CL, Skorych V, De Noni A Jr., Hotza D, Gómez González SY, Heinrich S, et al., Improving the sustainability of porcelain tile manufacture by flowsheet simulation. Ceram Int. 2023;49(14):24581-97. https://doi.org/10.1016/j.ceramint.2023.01.056
11. Alves CL, Skorych V, De Noni A Jr, Hotza D, González SYG, Heinrich S. Application of flowsheet simulation methodology to improve productivity and sustainability of porcelain tile manufacturing. Machines. 2023;11:137. https://doi.org/10.3390/machines11020137
12. Nassetti G, Ferrari F, Fregni A, Maestri G. Piastrelle Ceramiche & Energia: Banca dati dei consumi energetici nell' industria delle piastrelle di ceramica, Assopiastrelle, Bologna; 1998.
13. Li X, Ruan T, Hou K, Qu R. The configuring pathways of green technology advance, organizational strategy and policy environment for realizing low-carbon manufacturing from the perspective of simmelian tie: a qualitative comparative analysis of listed companies in China. J Cleaner Prod. 2023;382:135149.
14. Vieira AW, Rosso LS, Demarch A, Pasini D, Ruzza SP, Arcaro S, et al. Life cycle assessment in the ceramic tile industry: a review J Mater Res Technol. 2023;23:3904–15.
15. Mezquita A, Monfort E, Ferrer S, Gabaldón-Estevan D. How to reduce energy and water consumption in the preparation of raw materials for ceramic tile manufacturing: dry versus wet route. J Cleaner Prod. 2017;168:1566–70. https://doi.org/10.1016/j.jclepro.2017.04.082
16. Torres P, Manjate RS, Quaresma S, Fernandes HR, Ferreira JMF. Development of ceramic floor tile compositions based on quartzite and granite sludges. J Eur Ceram Soc. 2007;27:4649–55. https://doi.org/10.1016/j.jeurceramsoc.2007.02.217
17. Tarhan B, Tarhan M, Aydin T. Reusing sanitaryware waste products in glazed porcelain tile production. Ceram Int. 2017;43:3107–12. https://doi.org/10.1016/j.ceramint.2016.11.123
18. Alves CL, De Noni A Jr, Janssen R, Hotza D, Rodrigues Neto JB, Gómez González SY, et al. Integrated process simulation of porcelain stoneware manufacturing using flowsheet simulation. CIRP J Manuf Sci Technol. 2021;33:473–87. https://doi.org/10.1016/j.cirpj.2021.04.011
19. Skorych V, Dosta M, Hartge E-U, Heinrich S. Novel system for dynamic flowsheet simulation of solids processes. Powder Technol. 2017;314:665–79. https://doi.org/10.1016/j.powtec.2017.01.061
20. Skorych V, Dosta M, Heinrich S. Dyssol—an open-source flowsheet simulation framework for particulate materials. SoftwareX. 2020;12:100572. https://doi.org/10.1016/j.softx.2020.100572
21. Brasileiro CT, Conte S, Contartesi F, Melchiades FG, Zanelli C, Dondi M, et al. Effect of strong mineral fluxes on sintering of porcelain stoneware tiles. J Eur Ceram Soc. 2021;41:5755–67. https://doi.org/10.1016/j.jeurceramsoc.2021.04.027
22. Conte S, Zanelli C, Ardit M, Cruciani G, Dondi M. Phase evolution during reactive sintering by viscous flow: disclosing the inner workings in porcelain stoneware firing, J Eur Ceram Soc. 2020;40:1738–52. https://doi.org/10.1016/j.jeurceramsoc.2019.12.030
23. Amorós JL, Blasco E, Moreno A, Feliu C. Kinetics of the transformations occurring during the firing process of an industrial spray-dried porcelain stoneware body. Ceram Int. 2022;48:17611–20. https://doi.org/10.1016/j.ceramint.2022.03.031
24. dos Santos Conserva LR, Melchiades FG, Nastri S, Boschi AO, Dondi M, Guarini G, et al. Pyroplastic deformation of porcelain stoneware tiles: wet vs. dry processing. J Eur Ceram Soc. 2017;37:333–42. https://doi.org/10.1016/j.jeurceramsoc.2016.08.015
25. Haffez GSA. Correlation between work index and mechanical properties of some Saudi ores. Mater Test. 2012;54:108–12.
26. Dondi M, Ercolani G, Melandri C, Mingazzini C, Marsigli M. The chemical composition of porcelain stoneware tiles and

its influence on microstructural and mechanical properties. Interceram. 1999;48:75–83.
27. Perry JH. Chemical engineers' handbook. ACS Publications; 1950.
28. Tsakalakis KG, Stamboltzis GA. Modelling the specific griding energy and abll- mill scaleup. IFAC Proc. 2004;37:53–58.
29. Morrell. Power draw of wet tumbling mills and its relationship to charge dynamics. Part 1: A continuum approach to a mathematical modelling of mill power draw. Miner Process Extr Metall. 1996;105:C43–C53.
30. Walzel P. Spraying and atomizing of liquids, Ullmann's encyclopedia of industrial chemistry. Wiley-VCH; 2012. p. 79–98.
31. Ali M, Mahmud T, Heggs PJ, Ghadiri M, Djurdjevic D, Ahmadian H, et al. A one-dimensional plug flow model of a counter current spray drying tower. Chem Eng Res Des. 2014;92(5):826–41.
32. Balshin MY. Theory of compacting, Metalloprom. 1938;18:124–37.
33. Darolt R D, Cargnin M, Peterson M, De Noni A. Additional high-energy milling to enhance the performance of porcelain stoneware manufacturing. Int J Appl Ceram Technol. 2020;17:1742–51. https://doi.org/10.1111/ijac.13478
34. Khalili K, Bagherian M, Khisheh S. Numerical simulation of drying ceramic using finite element and machine vision. Proc Technol. 2014;12:388–93.
35. Kriaa W, Bejaoui S, Mhiri H, Palec G Le, Bournot P. Study of dynamic structure and heat and mass transfer of a vertical ceramic tiles dryer using CFD simulations. Heat Mass Transfer. 2014;50:235–51.
36. Gómez SY, Hotza D. Predicting powder densification during sintering. J Eur Ceram Soc. 2018;38:1736–41. https://doi.org/10.1016/j.jeurceramsoc.2017.10.020
37. De Noni A, Hotza D, Soler VC, Vilches ES. Effect of quartz particle size on the mechanical behaviour of porcelain tile subjected to different cooling rates. J Eur Ceram Soc. 2009;29:1039–46. https://doi.org/10.1016/j.jeurceramsoc.2008.07.052
38. Sacmi Iberica SA. Tecnología cerámica aplicada. Vol I, Faenza Editrice Ibérica SL Faenza RA, Italia: Litográfica Faenza SRL; 2001.
39. van Gelder A. Tecnología cerámica aplicada, Volumen II, SACMI; 2004.
40. Melchiades F G, Canavesi A, Boschi A O. Dimensionamento de Revestimentos Cerâmicos Visando a Maximização da Produtividade (Por que os Revestimentos tem os Tamanhos que tem?). Cerâm Ind. 2006;3:13–15.
41. SACMI, Asociación Española de Técnicos Cerámicos, Tecnología cerámica aplicada, Castellón de la Plana: Faenza Editrice Iberica; 2004
42. Ros-Dosdá T, Fullana-i-Palmer P, Mezquita A, Masoni P, Monfort E. How can the European ceramic tile industry meet the EU's low-carbon targets? A life cycle perspective. J Cleaner Prod. 2018;199:554–64. https://doi.org/10.1016/j.jclepro.2018.07.176
43. Peng J, Zhao Y, Jiao L, Zheng W, Zeng L. CO_2 Emission calculation and reduction options in ceramic tile manufacture—the Foshan case. Energy Procedia. 2012;16:467–76. https://doi.org/10.1016/j.egypro.2012.01.076
44. Nowtricity. CO_2 emissions per kWh in Spain. 2022. https://www.nowtricity.com/country/spain/. Accessed 27 Apr 2023
45. Ember. Low-carbon power ranking Brazil: 86.1% low-carbon power. 2022. https://lowcarbonpower.org/region/Brazil
46. Runst P, Höhle D. The German eco tax and its impact on CO_2 emissions. Energy Policy. 2022;160:112655. https://doi.org/10.1016/j.enpol.2021.112655
47. Bengochea-Morancho A, Higón-Tamarit F, Martínez-Zarzoso I. Economic growth and CO_2 emissions in the European Union. Environ Resour Econ. 2001;19:165–72. https://doi.org/10.1023/A:1011188401445
48. Magagnin D, dos Santos C M F, Wanderlind A, Jiusti J, De Noni A Jr. Effect of kaolinite, illite and talc on the processing properties and mullite content of porcelain stoneware tiles. Mater Sci Eng A. 2014;618:533–39. https://doi.org/10.1016/j.msea.2014.09.049
49. Wu J, Tian K, Wu C, Yu J, Wang H, Song J, et al. Effect of talc on microstructure and properties of the graphite tailing stoneware tiles. Constr Build Mater. 2021;311:125314. https://doi.org/10.1016/j.conbuildmat.2021.125314
50. Soldati R, Zanelli C, Guarini G, Fazio S, Bignozzi MC, Dondi M. Characteristics and rheological behaviour of spray-dried powders for porcelain stoneware slabs. J Eur Ceram Soc. 2018;38:4118–26. https://doi.org/10.1016/j.jeurceramsoc.2018.04.042
51. Santos D, Maurício AC, Sencadas V, Santos J D, Fernandes MH, Gomes PS. Spray drying: an overview. Biomaterials-Physics and Chemistry, New ed. 2018:9–35.
52. Iranfar S, Karbala MM, Shakiba M, Shahsavari MH. Effects of type and distribution of clay minerals on the physico-chemical and geomechanical properties of engineered porous rocks. Sci Rep. 2023;13:5837.
53. Meng L, Han L, Zhu H, Dong W, Li W, Bao Y. Influence of moisture content on the structural characteristics of argillaceous weakly consolidated rock caused by dynamic loading in the coal mine. Shock Vibration. 2021;2021:7206801. https://doi.org/10.1155/2021/7206801
54. Zheng W, Cui T, Li H, Yang Y. Novel dry-suspension granulation process for preparing pressed powders of ceramic tiles. Powder Technol. 2021;377:274–80. https://doi.org/10.1016/j.powtec.2020.09.003
55. Miranda GV, Rodrigues Neto JB, Bernardin AM. Hydro deformation in ceramic tiles at the pre-firing stage. J Eur Ceram Soc. 2021;41:7311–20. https://doi.org/10.1016/j.jeurceramsoc.2021.07.052
56. Pinter J Jr, Zaccaron A, Arcaro S, Neto JBR, De Noni A Jr, Pereira FR. Novel approach to ensure the dimensional stability of large-format enameled porcelain stoneware tiles through water absorption control. Open Ceram. 2022;9:100203. https://doi.org/10.1016/j.oceram.2021.100203
57. Santos-Barbosa D, Hotza D, Boix J, Mallol G, Deus A. Modelling the influence of manufacturing process variables on dimensional changes of porcelain tiles. Adv Mater Sci Eng. 2013;2013:142343. https://doi.org/10.1155/2013/142343
58. Ishizaki K, Komarneni S, Nanko M. Powder compacts and green bodies for porous materials. Porous Mater. 1998;4:12–37. https://doi.org/10.1007/978-1-4615-5811-8_2
59. Akdogan NE, Arioz E, Kockar OM. Investigation of physico-mechanical properties and multi-objective optimization of industrial ceramic tiles using response surface method: sintering temperature and time. Trans Indian Ceram Soc. 2023;82(3):177–86.

60. Castellano J, Sanz V, Canas E, Sánchez E. Industry-scalable wall tile composition based on circular economy Industry-scalable wall tile composition based on circular economy. Bol Soc Españ Cerám Vidrio. 2022;61:374–82.

How to cite this article: Alves CL, Skorych V, De Noni A, Hotza D, González SYG, Heinrich S. Optimizing raw material composition to increase sustainability in porcelain tile production: A simulation-based approach. J Am Ceram Soc. 2023;1–18. https://doi.org/10.1111/jace.19581

APPENDIX: RELATIONSHIP BETWEEN TOTAL COSTS AND CO2 EMISSIONS CONCERNING RAW MATERIAL COSTS

The dependence of CO_2 emissions for the various simulated raw material combinations according to the scenario of Spain ($C_{pr\ 2,Spain}$) and Brazil ($C_{pr\ 2,Brazil}$) can be seen in Figures A1 and A2, respectively:

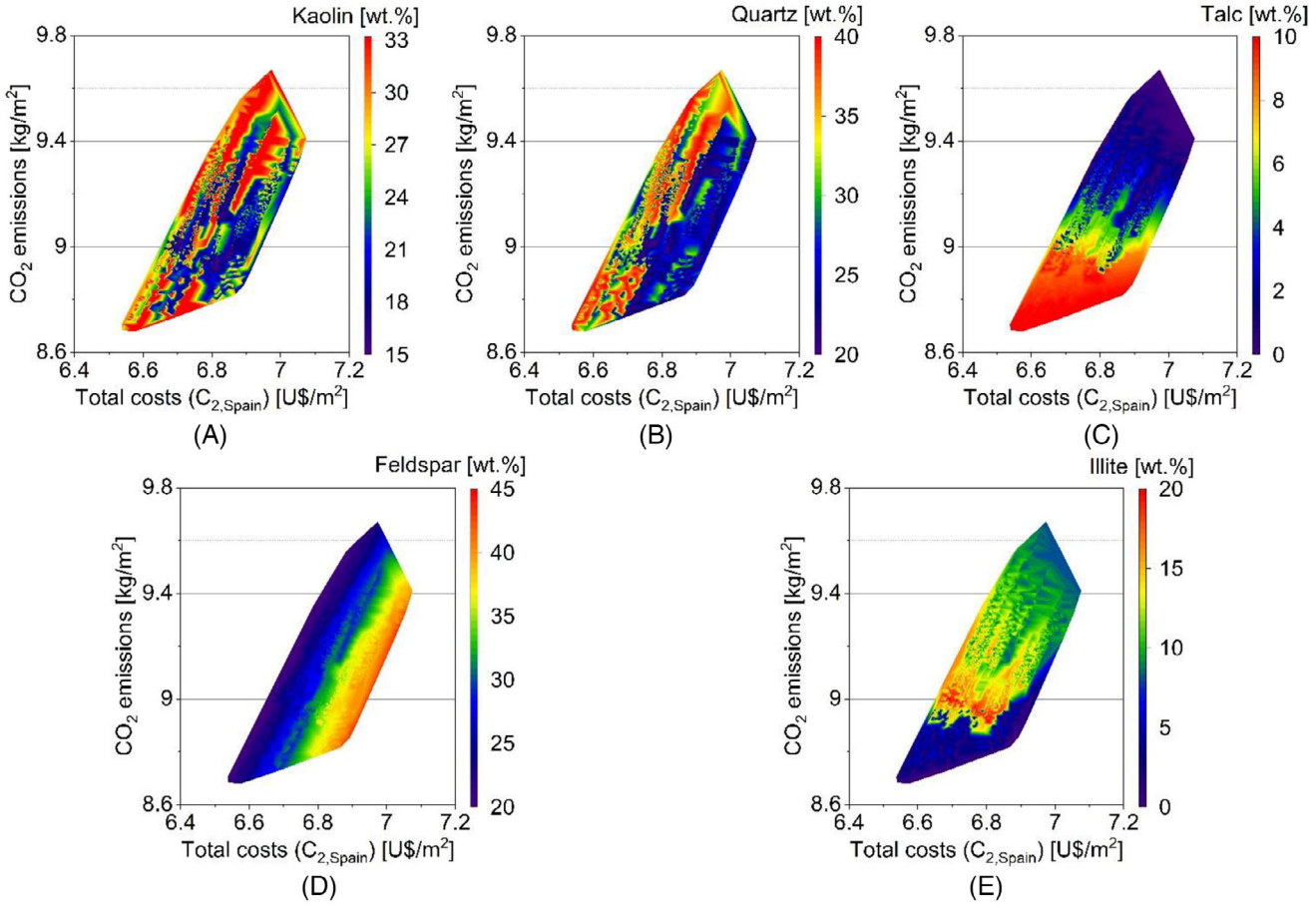

FIGURE A1 Comparison of total costs of production with CO_2 emissions considering different values of raw material costs for Spain ($C_{pr\ 2,Spain}$).

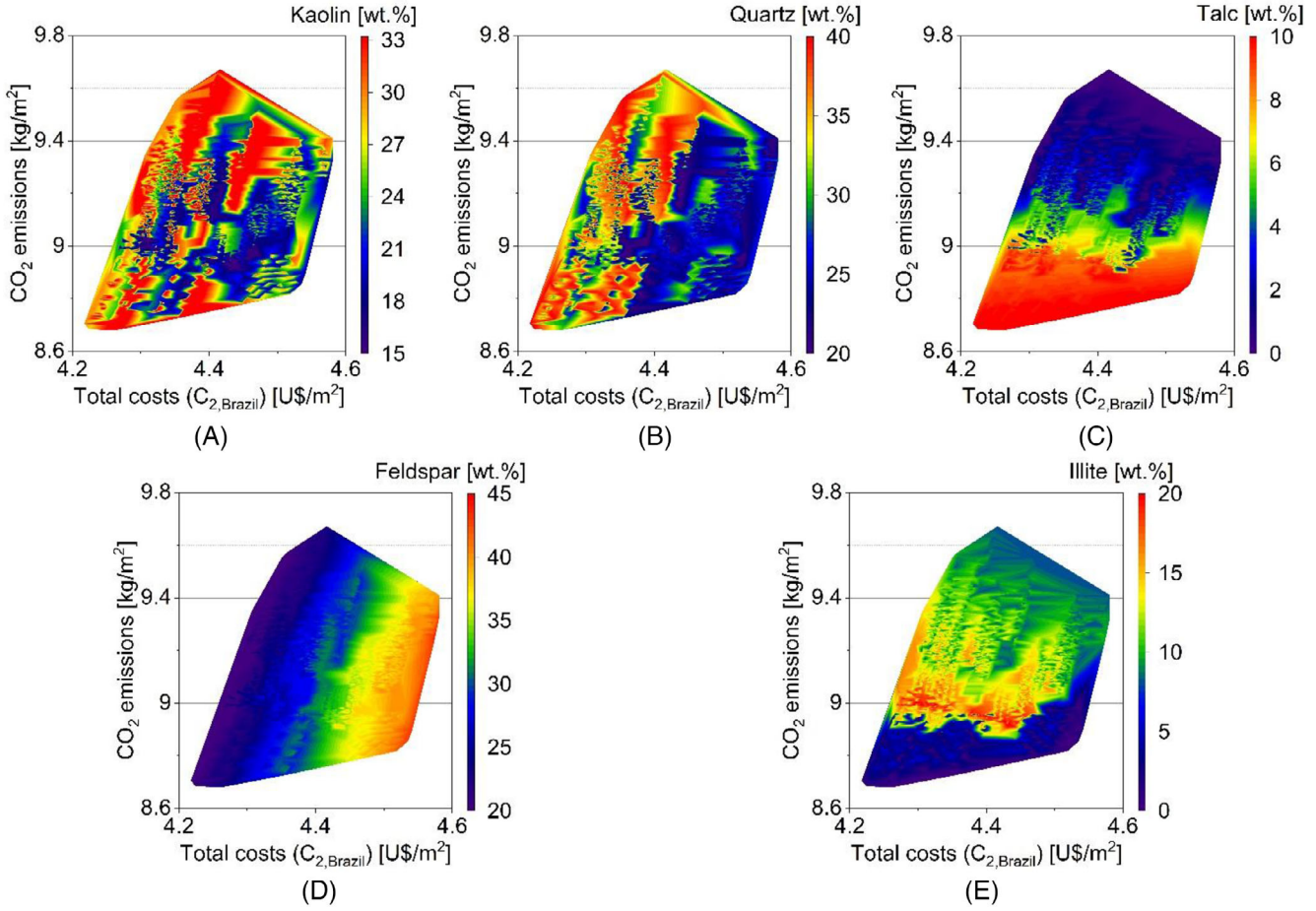

FIGURE A2 Comparison of total costs of production with CO_2 emissions considering different values of raw material costs for Brazil ($C_{\text{pr 2,Brazil}}$).